

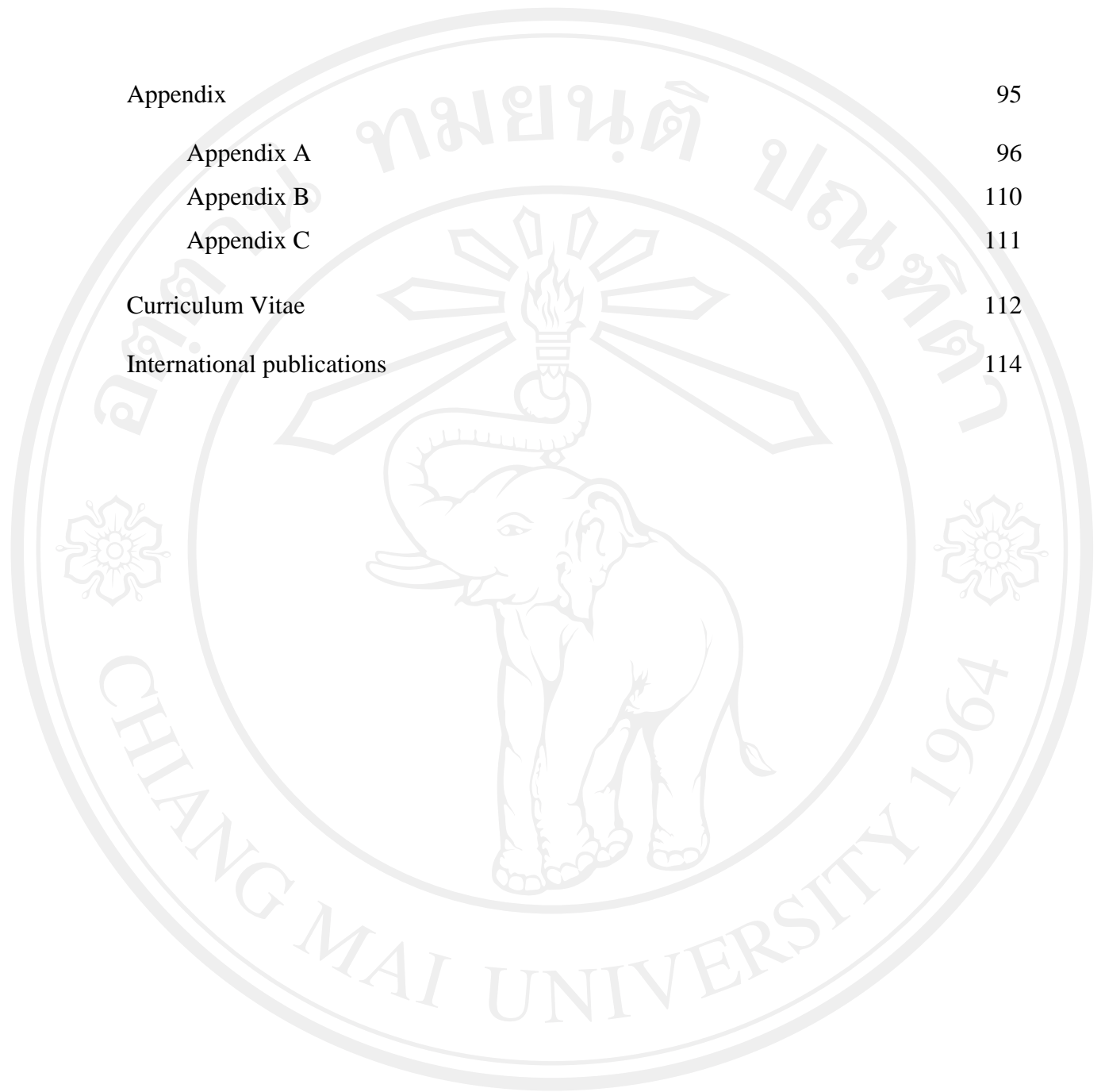
CONTENTS

	Page
Acknowledgement	d
Abstract in Thai	e
Abstract in English	g
List of Tables	m
List of Figures	n
List of Abbreviations	r
List of Symbols	t
Statement of Originality	u
Chapter 1 Introduction	1
1.1 Research Objectives	4
1.2 Usefulness of the Research	4
Chapter 2 Literature Review	5
2.1 Crystalline structure, properties and application of metal oxides	5
2.1.1 MoO ₃	5
2.1.2 CuO	8
2.2 Microwave synthesis	12
2.2.1 Introduction	12
2.2.2 Microwave heating	14
1). Microwave versus conventional heating	14
2). Interaction of microwave with materials	15
2.3 Microwave plasma	21
2.3.1 Power transfer to the plasma	21

	Page
2.3.2 microwave plasma application for materials synthesis	24
2.4 DC electrical heating	29
2.4.1 Direct current heating method	29
2.4.2 Basic configuration of the system	29
2.4.3 DC pulse current energizing effect	30
2.4.4 Synthesis by using direct electrical current heating method	31
2.5 Gas sensor based on metal oxide semiconductor	32
Chapter 3 Experimental Procedure	37
3.1 Chemical reagents and equipment	37
3.1.1 Chemical reagents	37
3.1.2 Equipment	37
3.2 Experimental procedure	38
3.2.1 MoO ₃ : Synthesis using plasma microwave method and optical characterization	38
1) Synthesis of MoO ₃	38
2) Characterization	39
3.2.2 CuO: Synthesis using DC electrical heating method, characterization and gas sensing measurement	40
1). Synthesis of CuO	40
2). Characterization	40
3). Fabrication and measurement of sensor	41
3.3 Characterization techniques	43
3.3.1 X-ray diffraction	43
3.3.2 Scanning electron microscopy	44
3.3.3 TEM, HRTEM and SAED	45
3.3.4 Luminescence spectroscopy	46
3.3.5 UV-Vis spectroscopy	47
3.3.6 Raman spectrometry	48

	Page
3.3.7 Fourier transform infrared spectroscopy	48
3.3.8 System source meter	49
3.3.9 X-ray photoelectron spectroscopy	49
3.3.9 High DC electrical power supply	50
Chapter 4 Results and Discussion	51
4.1 MoO ₃	51
4.1.1 XRD, SAED, and HRTEM	51
4.1.2 SEM	53
4.1.3 Raman and FTIR analyses	56
4.1.4 PL emission	58
4.2 CuO	59
4.2.1 XRD	59
4.2.2 TEM and SEM	62
4.2.3 FTIR	67
4.2.4 PL and UV-Vis	68
4.2.5 XPS	70
4.2.5 V-I Characteristic Curve	72
4.2.6 Gas Sensing Measurement	73
Chapter 5 Conclusions	79
References	82
List of publications	94

	Page
Appendix	95
Appendix A	96
Appendix B	110
Appendix C	111
Curriculum Vitae	112
International publications	114



ลิขสิทธิ์มหาวิทยาลัยเชียงใหม่
Copyright© by Chiang Mai University
All rights reserved

LIST OF TABLES

	Page	
Table 2.1	Some physical properties of MoO ₃	7
Table 2.2	Structural parameters of CuO	9
Table 2.3	Key physical properties of CuO at room temperature (300 K)	10
Table 2.4	Microwave-Active Elements, Natural Minerals, and Compounds	19
Table B.1	Camera constant ($L\lambda$) at 200 kV of JEOL-TEM	109
Table B.2	NH ₃ gas flow rate controlled by gas regulator (Cole-Parmer model PMR 1-010333)	110

LIST OF FIGURES

		Page
Figure 2.1	The structures [36] of a) α -MoO ₃ , b) ReO ₃ and c) unit cell for the lattice of ReO ₃ . The octahedral symmetry is emphasized in c)	6
Figure 2.2	Crystal structure of CuO (tenorite). The special atomic positions for Cu are (1/4, 1/4, 0), (3/4, 3/4, 0), (1/4, 3/4, 1/2), and (3/4, 1/4, 1/2) and for oxygen are (0, y, 1/4), (0, 1/2 + y, 1/4), (0, -y, 3/4), and (1/2, 1/2 - y, 3/4) with y = 0.416(2). The small light spheres and large dark spheres represent Cu and oxygen atoms, respectively.	8
Figure 2.3	(a and b) Optical images of CuO nanobelt-based two-layered SWCNTs and CuO nanobelts mixed with SWCNT (9:1 weight ratio) electrode. (c) Edge of SWCNTs and CuO nanobelts. (d) Galvanostatic charge/discharge curves measured with a current density of 5 A/g for different electrodes. (e) Cycling performance for SWCNTs and CuO nanobelts mixed with SWCNT electrode at a current density of 5 A/g in 1.0 M LiPF ₆ /EC: DEC.	11
Figure 2.4	Composition of electromagnetic wave	12
Figure 2.5	Electromagnetic spectrum and it's interaction with molecule	13
Figure 2.6	Comparison heating mechanism between conventional and microwave oven	15
Figure 2.7	Heating mechanism of water due to microwave field.	20
Figure 2.8	Schematic diagram of Cober microwave system used in the synthesis of binary nitride materials by reaction with a nitrogen plasma.	25
Figure 2.9	Schematic diagram of (a) the apparatus for plasma modification by making use of an atmospheric microwave plasma torch and (b) the construction of the plasma nozzles.	26

	Page	
Figure 2.10	A photograph of the microwave plasma in operation for the treatment of Al sample.	27
Figure 2.11	Schematic presentation of the synthetic system of MgO nanoparticles with the atmospheric microwave plasma torch. The inset shows the plasma emission of green color after completion of the synthesis.	28
Figure 2.12	A schematic diagram of microwave plasma equipment	29
Figure 2.13	A schematic diagram of direct current heating method apparatus	30
Figure 2.14	Pulsed current flow through powder particles	31
Figure 2.15	Schematic diagram for change of the sensor resistance upon exposure to the reducing gas in the cases of n-type and p-type MOS sensors	34
Figure 2.16	Formation of electronic core–shell structures in (a) n-type and (b) p-type oxide semiconductors	35
Figure 3.1	Schematic diagram of microwave induced plasma system.	39
Figure 3.2	Schematic diagram of lab-made DC electrical heating method	42
Figure 3.3	Diagram of lab-made gas sensing measurement system	42
Figure 3.4	Picture of lab-made gas sensing measurement system	43
Figure 3.5	X-ray diffractometer	44
Figure 3.6	Scanning electron microscope	45
Figure 3.7	Transmission electron microscope	46
Figure 3.8	Luminescence spectrometer	47
Figure 3.9	UV-VIS spectrophotometer	47
Figure 3.10	Raman spectroscopy	48
Figure 3.11	Fourier transform infrared spectroscope	48
Figure 3.12	System source meter	49
Figure 3.13	X-ray photoelectron spectrometer	50
Figure 3.14	High DC current power supply	50

	Page	
Figure 4.1	Diffractogram of processed α -MoO ₃ for 40, 50, and 60 min	52
Figure 4.2	a) SAED pattern and b) HRTEM image of α -MoO ₃ processed for 60 min.	53
Figure 4.3	SEM images of MoO ₃ crystals processed for 40 min	54
Figure 4.4	SEM images of MoO ₃ crystals processed for 50 min	54
Figure 4.5	SEM images of MoO ₃ crystals processed for 60 min (x 1,000)	55
Figure 4.6	SEM images of MoO ₃ crystals processed for 60 min (x 5,000)	55
Figure 4.7	a) Raman analysis of α -MoO ₃ processed for 40, 50 and 60 min. b) FTIR spectrum of α -MoO ₃ processed for 60 min.	57
Figure 4.8	PL emissions of α -MoO ₃ processed for 40, 50, and 60 min.	59
Figure 4.9	XRD patterns of the samples synthesized for 1, 3, 6, 9, 12 and 15 min processing times.	61
Figure 4.10	TEM image of the 15 min as-synthesized CuO sample and its simulated crystal structure.	62
Figure 4.11	SEM image of the sample synthesized for 1 min.	63
Figure 4.12	SEM image of the sample synthesized for 3 min.	64
Figure 4.13	SEM image of the sample synthesized for 6 min.	64
Figure 4.14	SEM image of the sample synthesized for 9 min.	65
Figure 4.15	SEM image of the sample synthesized for 12 min.	65
Figure 4.16	SEM image of the sample synthesized for 15 min.	66
Figure 4.17	FTIR spectra of the samples synthesized for 1, 3, 6, 9, 12 and 15 min processing times.	67
Figure 4.18	PL peaks of CuO processed at different length of time	69
Figure 4.19	Direct band gap estimation of 15 min synthesized CuO	70
Figure 4.20	XPS spectra of the 15 min as-synthesized CuO sample: (a) Cu 2p and (b) O 1s.	71
Figure 4.21	Symmetric current and voltage behavior for 15 min processed CuO at various temperature	73

Figure 4.22	Dynamic respond-recovery curve of 15 min synthesized CuO at different working temperature	74
Figure 4.23	Sensitivity of 15 min processed CuO at various working temperature	75
Figure 4.24	Current density characteristic of the 15 min as-synthesized CuO sample at different NH ₃ concentrations.	76
Figure 4.25	Sensitivity of the 15 min as-synthesized CuO sample at different NH ₃ concentrations.	77

LIST OF ABBREVIATIONS

A	Ampere
Å	Angstrom
a.u.	Arbitrary Unit
°C	Degree Celsius
cm	Centimeter
cm ³	Cubic centimeter
DC	Direct Current
deg	Degree
E _g	Energy Gap
eV	Electron Volt
FESEM	Field-Emission Scanning Electron Microscopy
FTIR	Fourier Transform Infrared Spectroscopy
FWHM	Full Width at Half Maximum
g	Gram
GHz	Gigahertz
HRTEM	High Resolution Transmission Electron Microscopy
I	current
JCPDS	Joint Committee on Powder Diffraction Standards
m	Meter
MHz	Magahertz
min	minute
NIR	Near-Infrared
nm	Nanometer
ppm	part per million
PL	Photoluminescense
s	Second
S	Sensitivity

SAED	Selected Area Electron Diffraction
TEM	Transmission Electron Microscopy
TGA	Thermogravimetric Analysis
UV	Ultraviolet
V	volt
vis	Visible
W	Watt
XRD	X-Ray Diffraction
μm	Micrometer

ลิขสิทธิ์มหาวิทยาลัยเชียงใหม่
Copyright© by Chiang Mai University
All rights reserved

LIST OF SYMBOLS

λ	wavelength
θ	theta
ϵ	permittivity
ϵ'	the real component of permittivity
ϵ''	the imaginary component of permittivity
m_e	the electron mass
ν_c	the average electron-neutral collision frequency
θ_A	power absorbed from the field per electron
α	absorption coefficient
ν	frequency

ลิขสิทธิ์มหาวิทยาลัยเชียงใหม่
Copyright© by Chiang Mai University
All rights reserved

ข้อความแห่งการริเริ่ม

- 1) วิทยานิพนธ์นี้ได้นำเสนอวิธีการสังเคราะห์โลหะออกไซด์ที่มีโครงสร้างระดับไมโครและนาโนเมตร ซึ่งสารกลุ่มโลหะออกไซด์ที่มีขนาดดังกล่าวสามารถนำมาประยุกต์ใช้งานได้หลากหลาย โดยแสดงสมบัติทั้งเชิงกายภาพและเคมีที่ดีกว่าสารชนิดเดียวกันที่มีโครงสร้างขนาดใหญ่ (bulk materials) โดยเฉพาะการนำมาใช้งานที่เกี่ยวข้องกับสมบัติทางแสงและการรับรู้ก๊าซ
- 2) ความบกพร่องบริเวณผิวของโครงสร้างโลหะออกไซด์ชนิดการเกิดที่ว่างของออกซิเจน เป็นผลให้สารสามารถตอบสนองการรับรู้ก๊าซได้ดียิ่งขึ้น โดยสามารถทำการวิเคราะห์ความบกพร่องดังกล่าวจากสมบัติทางแสงด้วยวิธีโฟโตลูมิเนสเซนส์
- 3) การใช้งานสารโลหะออกไซด์ที่มีโครงสร้างในระดับไมโครและนาโนเมตรมีแนวโน้มที่เพิ่มมากขึ้น ดังนั้นการศึกษาหาวิธีการสังเคราะห์ที่ง่าย รวดเร็ว และไม่มีของเสียจากการสังเคราะห์ จึงเป็นหัวข้อที่มีความสำคัญเป็นอย่างมาก ซึ่งเครื่องมือที่ถูกพัฒนาขึ้นมาโดยใช้หลักการให้ความร้อนด้วยคลื่นไมโครเวฟ และไฟฟ้ากระแสตรง นับเป็นวิธีที่มีความเหมาะสมสำหรับการสังเคราะห์ในลักษณะดังกล่าว

STATEMENT OF ORIGINALITY

- 1) In this thesis, metal oxides with micro- and nanostructured were presented their synthesizing method. Metal oxides in micro and nano scale can be used in a variety technological application and show a better properties both chemical and physical compare with the their bulk materials. Especially, optical and gas sensing application are widely applied.
- 2) Defect at the metal oxide surface , oxygen vacancy, is the cause to make a substance having a better gas response. The imperfect determination is examined by employing photoluminescence analytical method.
- 3) Metal oxides with micro- and nanostructured show a higher using by trend. Therefore, the low cost, simply, rapid and environmental friendly synthesizing method should be considered as an important topic of nanoscience and technology. Microwave and directly electrical applying technique are suitable processing for heat generation corresponding with the future trend of materials synthesis.